Research article

Dynamics of a coupled epileptic network with time delay

Yulin Guan and Xue Zhang[*]

College of Science, Northeastern University, Shenyang,110000, China

* **Correspondence:** Email: zhangxue@mail.neu.edu.cn.

Abstract: Epilepsy is considered as a brain network disease. Epileptic computational models are developed to simulate the electrophysiological process of seizure. Some studies have shown that the epileptic network based on those models can be used to predict the surgical outcome of patients with drug-resistant epilepsy. Most studies focused on the causal relationship between electrophysiological signals of different brain regions and its impact on seizure onset, and there is no knowledge about how time delay of electrophysiological signal transmitted between those regions related to seizure onset. In this study, we proposed an epileptic model with time delay between network nodes, and analyzed whether the time delay between nodes of epileptic network can cause seizure like event. Our results showed that the time delay between nodes may drive the network from normal state to seizure-like event through Hopf bifurcation. The time delay between nodes of epileptic computational network alone may induce seizure-like event. Our analysis suggested that the time delay of electrophysiological signals transmitted between different regions may be an important factor for seizure happening, which provide a deeper understanding of the epilepsy, and a potential new path for epilepsy treatment.

Keywords: epilepsy; stability; seizure-like event; Hopf bifurcation; time delay

1. Introduction

Epilepsy is a chronic brain disease, which is characterized by the occurrence of spontaneous seizures [1]. The affected neurons produce synchronized abnormal discharges during seizure [2]. There are about 50 million patients with epilepsy globally, and there are two million new patients each year. The focal onset seizure is the most common type for patient with epilepsy. The onset starts locally and propagates to normal brain tissues [3, 4]. There are interactions between pathological and normal brain regions [5]. The epilepsy is now considered as a brain network disease. The epileptic discharges are with complex temporal and spatial characteristics [6, 7]. How the seizure onselectroencephalogram (EEG)ets and propagates to neighbor regions is still in an infancy [8]. Some early studies proposed mathematical models to simulate the seizure onset, propagation and termination, which are critical to drug treatment, surgical intervention and neuromodulation of epilepsy [9, 10].

There are different approaches to model the epileptic behaviors of the brain. Wendling *et al*. introduced a computational macroscopic model of electroencephalogram (EEG) activity that included a physiologically relevant fast inhibitory feedback loop and the transition from interictal to fast ictal activity was explained by the impairment of dendritic inhibition in the model [11, 12]. Kalitzin *et al*. proposed an analytical model as examples of transitions between various dynamical states [13]. The model was then used to study the dynamics of convulsive seizure termination and postictal generalized EEG suppression [14]. Jirsa *et al*. proposed a generic model called Epileptor. They showed that the onset and offset of ictal-like discharges were well-defined mathematical events: a saddle-node and homoclinic bifurcation, respectively [15].

Furthermore, the coupled Epileptor network can be used to predict the spatiotemporal diversity of seizure propagation and termination in human focal epilepsy [16]. Time lags between epilepsy network nodes were considered as an important fact linked to seizure onset [17]. Bandt *et al*.

studied connectivity strength and time lags between different network nodes using resting-state functional Magnetic Resonance Imaging (fMRI). They showed that there were decreased time lags within the seizure onset node and globally increased time lags throughout all regions of the brain not involved in seizure onset or propagation [18].

In this study (see Figure 1), we investigated that the dynamical behaviors of epilepsy network based on simplified Epileptor model with time delay , and how the variation of time delay between the network nodes induce seizure-like event.

2. Local stability and Hopf bifurcation

The Epileptor model was introduced to represent complex behavior of the brain for patient with epilepsy. Taking advantage of time scale separation and focusing on the slower time scale, two dimensional Epileptor was proposed as follows [16]:

$$\begin{cases} \frac{dx_{1,i}}{dt} = -x_{1,i}^3 - 2x_{1,i}^2 + 1 - z_i + I_{1,i}, \\ \frac{dz_i}{dt} = \frac{1}{\tau_0}\left[4(x_{1,i} - x_{0,i}) - z_i - \sum_{j=1}^{N} K_{ij}(x_{1,j} - x_{1,i})\right], \end{cases}$$

where $i \in \{1,2\}$; characteristic time scale is fixed at $\tau_0 = 2857$, and resting-state current $I_{1,i} = 3.1$. $x_{1,i}$ is the state variables on the slower time scale account for spike and wave events observed in electrographic seizure recordings. z is the state variable which guides the neural population through the seizures including seizure onset and offset. K_{ij} is the connection strength between Epileptor i and Epileptor j as given by the connectivity matrix with $i, j = 1, 2$. The parameter $x_{0,i}$ describes the excitability degree of each Epileptor.

Some studies have shown that the time lags between different brain regions will change in patients with epilepsy. Proix $et\ al$ found delays of recruitment can be either highly variable or stereotypical by computing for several seizures the mean and SD of the delays of recruitment and the values of excitability and coupling parameters [8]. Zhang $et\ al$ found that time delay is related to coupled seizure network, which is unavoidably encountered due to finite speed, reaction time of signal transmission over the couplings, can lead to instabilities, bursting transitions, bifurcations of periodic [19]. In this paper, we consider

the following epileptic model with two time delays between coupled nodes:

$$\begin{cases} \frac{dx_{11}}{dt} = -x_{11}^3 - 2x_{11}^2 + 1 - z_1 + I_{11}, \\ \frac{dz_1}{dt} = \frac{1}{\tau_0}\left[4(x_{11} - x_{01}) - z_1 - K_{12}(x_{12}(t - \tau_1) - x_{11})\right], \\ \frac{dx_{12}}{dt} = -x_{12}^3 - 2x_{12}^2 + 1 - z_2 + I_{12}, \\ \frac{dz_2}{dt} = \frac{1}{\tau_0}\left[4(x_{12} - x_{02}) - z_2 - K_{21}(x_{11}(t - \tau_2) - x_{12})\right]. \end{cases}$$
(2.1)

The nontrivial equilibrium point of model system (2.1) is $P(x_{11}^*, z_1^*, x_{12}^*, z_2^*)$, where

$$z_1^* = -x_{11}^{*3} - 2x_{11}^{*2} + 1 + I_{11},$$

$$x_{12}^* = \frac{x_{11}^{*3} + 2x_{11}^{*2} + (4 + K_{12})x_{11}^* - 4x_{01} - 1 - I_{11}}{K_{12}},$$

$$z_2^* = -x_{12}^{*3} - 2x_{12}^{*2} + 1 + I_{12},$$

and x_{11}^* satisfies the following equation:

$$K_{21}x_{11} - h^3(x_{11}) - 2h^2(x_{11}) - (4 + K_{21})h(x_{11}) + 4x_{02} + I_{12} + 1 = 0,$$

where

$$h(x_{11}) = \frac{x_{11}^3 + 2x_{11}^2 + (4 + K_{12})x_{11} - 4x_{01} - 1 - I_{11}}{K_{12}}.$$

The characteristic equation of model (2.1) at the nontrivial equilibrium point P is given by:

$$|\lambda I - J| = \begin{vmatrix} \lambda + 3x_{11}^{*2} + 4x_{11}^* & 1 & 0 & 0 \\ -\frac{4+K_{12}}{\tau_0} & \lambda + \frac{1}{\tau_0} & \frac{K_{12}e^{-\lambda\tau_1}}{\tau_0} & 0 \\ 0 & 0 & \lambda + 3x_{12}^{*2} + 4x_{12}^* & 1 \\ \frac{K_{21}e^{-\lambda\tau_2}}{\tau_0} & 0 & -\frac{4+K_{21}}{\tau_0} & \lambda + \frac{1}{\tau_0} \end{vmatrix},$$

which can be reduced into the following form

$$\lambda^4 + A_1\lambda^3 + A_2\lambda^2 + A_3\lambda + A_4 + A_5 e^{-\lambda\tau_1 - \lambda\tau_2} = 0, \quad (2.2)$$

where

$A_1 = 3x_{11}^{*2} + 3x_{12}^{*2} + 4x_{11}^* + 4x_{12}^* + \frac{2}{\tau_0}$,

$A_2 = (3x_{11}^{*2} + 4x_{11}^*)(3x_{12}^{*2} + 4x_{12}^*) + \frac{6x_{11}^{*2} + 6x_{12}^{*2} + 8x_{11}^* + 8x_{12}^* + K_{12} + K_{21} + 8}{\tau_0} + \frac{1}{\tau_0^2}$,

$A_3 = \frac{(3x_{11}^{*2} + 4x_{11}^*)(6x_{12}^{*2} + 8x_{12}^* + K_{21} + 4)}{\tau_0} + (3x_{12}^{*2} + 4x_{12}^*)$

$\cdot \frac{4 + K_{12}}{\tau_0} + \frac{3x_{11}^{*2} + 3x_{12}^{*2} + 4x_{11}^* + 4x_{12}^* + K_{12} + K_{21} + 8}{\tau_0^2}$,

$A_4 = \frac{(3x_{11}^{*2} + 4x_{11}^*)(3x_{12}^{*2} + 4x_{12}^* + K_{21} + 4) + (4 + K_{12})(4 + K_{21} + 3x_{12}^{*2} + 4x_{12}^*)}{\tau_0^2}$,

$A_5 = -\frac{K_{12}K_{21}}{\tau_0}$.

When $\tau_1 = \tau_2 = 0$, the characteristic equation (2.2) becomes

$$\lambda^4 + A_1\lambda^3 + A_2\lambda^2 + A_3\lambda + A_4 + A_5 = 0.$$
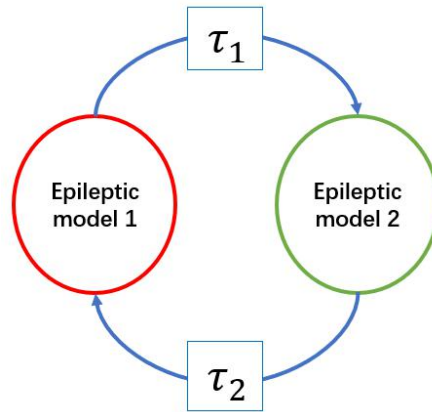
Figure 1. The epilepsy network with double time delay.

According to Routh-Hurwitz criteria, the positive equilibrium of model (2.1) in the absence of time delay is locally asymptotically stable when the following conditions are satisfied:

$$A_1 > 0, \ A_1A_2 - A_3 > 0 \text{ and } A_3(A_1A_2 - A_3) > A_1^2(A_4 + A_5) > 0. \quad (2.3)$$

Next, we will analyze the effects of the two time-delays on the stability of the nontrival equilibrium point P. We substitute $i\omega$ into equation(2.2) and separate the real and imaginary parts, then we obtain the following equations:

$$\begin{cases} \omega^4 - A_2\omega^2 + A_4 = -A_5\cos(\omega(\tau_1 + \tau_2)), \\ -A_1\omega^3 + A_3\omega = A_5\sin(\omega(\tau_1 + \tau_2)), \end{cases} \quad (2.4)$$

from which it follows that

$$\omega^8 + (A_1^2 - 2A_2)\omega^6 + (2A_4 + A_2^2 - 2A_1A_3)\omega^4 + \\ (A_3^2 - 2A_2A_4)\omega^2 + A_4^2 - A_5^2 = 0. \quad (2.5)$$

If $A_4^2 - A_5^2 < 0$, the Equation (2.5) has a positive real root ω_0^*. We define $\tau = \tau_1 + \tau_2$, then we get

$$\tau_k^* = \frac{1}{\omega_0^*} \arccos \frac{\omega_0^{*4} - A_2\omega_0^{*2} + A_4}{-A_5} + \frac{2k\pi}{\omega_0^*}, k = 0, 1, 2...$$

According to the Butler's Lemma, we can conclude that the equilibrium point P is stable for $\tau < \tau_0^*$. Now, we discuss whether Hopf bifurcation occurs at P of model (2.1) when τ increases through τ_0^*.
Based on Equation (2.2), we can further obtain

$$\begin{aligned} \text{Sign}\Big(\frac{d}{d\tau}\text{Re}(\lambda)\Big)\,|_{\tau_k^*} &= \text{Sign}\Big(\text{Re}(\frac{d\lambda}{d\tau})^{-1}\Big)\,|_{\tau_k^*} \\ &= \text{Sign}\Big(4\omega_0^{*6} + (3A_1^2 - 6A_2)\omega_0^{*4} \\ &\quad + (2A_2^2 - 4A_1A_3 + 4A_4)\omega_0^{*2} \\ &\quad + A_3^2 - 2A_2A_4\Big). \end{aligned} \quad (2.6)$$

From Equation (2.6), it is clear that the sign can be determined by

$$\text{Sign}\left(f'(x)\,|_{x=\omega_0^{*2}}\right),$$

where $f(x) = x^4 + (A_1^2 - 2A_2)x^3 + (2A_4 + A_2^2 - 2A_1A_3)x^2 + (A_3^2 - 2A_2A_4)x + A_4^2 - A_5^2$.

Theorem 1 Assume that the conditions in (2.3), $A_4^2 - A_5^2 < 0$ and $f'(\omega_0^{*2}) \neq 0$ hold. The equilibrium point P of model (2.1) is locally asymptotically stable for $\tau \in [0, \tau_0^*)$, and Hopf bifurcation occurs at P when $\tau = \tau_0^*$, where

$$\tau_0^* = \frac{1}{\omega_0^*} \arccos \frac{\omega_0^{*4} - A_2\omega_0^{*2} + A_4}{-A_5}.$$

3. Stability of bifurcated periodic solutions

Generally speaking, the time delays between two network nodes are always similar, so we consider a special case $\tau_1 = \tau_2$. In what follows, we will investigate the direction of Hopf bifurcation, stability and period of the periodic solution bifurcating from the equilibrium point P. Following the ideas of Hassard et al. [20], we derive the explicit formulae for determining these properties of Hopf bifurcation at the critical value $\tau_s^* = \frac{\tau_0^*}{2}$ by employing the normal form method

and center manifold theorem. Let

$$u_1 = x_{11} - x_{11}^*,$$
$$u_2 = z_1 - z_1^*,$$
$$u_3 = x_{12} - x_{12}^*,$$
$$u_4 = z_2 - z_2^*,$$

and $u_1(t) = x_{11}(\tau_s t), u_2(t) = z_1(\tau_s t), u_3(t) = x_{12}(\tau_s t), u_4(t) = z_2(\tau_s t), \tau_s = \tau_s^* + \mu, \mu \in R$. For system(2.1), $\mu = 0$ is the Hopf bifurcation value. In the fixed phase space $C = C([-1, 0], R^4)$, system (2.1) is transformed into a FDE as

$$\dot{u}(t) = L_\mu(u_t) + F(\mu, u_t), \qquad (3.1)$$

where $u(t) = (u_1(t), u_2(t), u_3(t), u_4(t))^T \in R^4$, and $L_\mu : C \to R, F : R \times C \to R$ are given respectively by

$$L_\mu(\phi) =$$

$$(\tau_s^* + \mu)(\begin{pmatrix} -3x_{11}^{*2} - 4x_{11}^* & -1 & 0 & 0 \\ \frac{4+K_{12}}{\tau_0} & -\frac{1}{\tau_0} & 0 & 0 \\ 0 & 0 & -3x_{12}^{*2} - 4x_{12}^* & -1 \\ 0 & 0 & \frac{4+K_{21}}{\tau_0} & -\frac{1}{\tau_0} \end{pmatrix}$$

$$\cdot \phi(0) + \begin{pmatrix} 0 & 0 & 0 & 0 \\ 0 & 0 & -\frac{K_{12}}{\tau_0} & 0 \\ 0 & 0 & 0 & 0 \\ -\frac{K_{21}}{\tau_0} & 0 & 0 & 0 \end{pmatrix} \phi(-1))$$

and

$$F(\mu, \phi) = (\tau_s^* + \mu) \begin{pmatrix} (-3x_{11}^* - 2)\phi_1^2(0) - \phi_1^3(0) \\ 0 \\ (-3x_{12}^* - 2)\phi_3^2(0) - \phi_3^3(0) \\ 0 \end{pmatrix},$$

$$(3.2)$$

where $\phi(\theta) = (\phi_1(\theta), \phi_2(\theta), \phi_3(\theta), \phi_4(\theta))^T \in C$.

According to the Riesz representation theorem, there exists a 4×4 matrix $\eta(\theta, \mu)$ of bounded variation for $\theta \in [-1, 0]$, which follows that

$$L_\mu \phi = \int_{-1}^{0} d\eta(\theta, \mu)\phi(\theta), \text{ for } \phi \in \mathrm{C}.$$

In fact, we can choose

$$\eta(\theta, \mu) = \begin{cases} (\tau_s^* + \mu) \begin{pmatrix} -3x_{11}^{*2} - 4x_{11}^* & -1 & 0 & 0 \\ \frac{4+K_{12}}{\tau_0} & -\frac{1}{\tau_0} & -\frac{K_{12}}{\tau_0} & 0 \\ 0 & 0 & -3x_{12}^{*2} - 4x_{12}^* & -1 \\ -\frac{K_{21}}{\tau_0} & 0 & \frac{4+K_{21}}{\tau_0} & -\frac{1}{\tau_0} \end{pmatrix}, \\ \hspace{4cm} \theta = 0, \\ (\tau_s^* + \mu) \begin{pmatrix} 0 & 0 & 0 & 0 \\ 0 & 0 & -\frac{K_{12}}{\tau_0} & 0 \\ 0 & 0 & 0 & 0 \\ -\frac{K_{21}}{\tau_0} & 0 & 0 & 0 \end{pmatrix}, \theta \in (-1, 0), \\ 0_{4\times4}, \hspace{2.2cm} \theta = -1. \end{cases}$$

For $\phi \in C^1([-1, 0], R^4)$, we define

$$A(\mu)\phi = \begin{cases} \frac{d\phi(\theta)}{d\theta}, & -1 \le \theta < 0, \\ \int_{-1}^{0} d\eta(s, \mu)\phi(s), & \theta = 0, \end{cases}$$

and

$$R(\mu)\phi = \begin{cases} 0, & -1 \le \theta < 0, \\ F(\mu, \phi), & \theta = 0. \end{cases}$$

Then system (3.1) is equivalent to

$$\dot{u}_t = A(\mu)u_t + R(\mu)u_t, \qquad (3.3)$$

where $u_t(\theta) = u(t + \theta)$, for $\theta \in [-1, 0]$.
For $\psi \in C^1([0, 1], (R^4)^*)$, we define

$$A^*\psi(s) = \begin{cases} -\frac{d\psi(s)}{ds}, & s \in (0, 1], \\ \int_{-1}^{0} d\eta^T(t, 0)\psi(-t), & s = 0, \end{cases}$$

and the bilinear form

$$\langle \psi(s), \phi(\theta) \rangle = \overline{\psi}(0)\phi(0) - \int_{-1}^{0} \int_{\xi=0}^{\theta} \overline{\psi}(\xi - \theta)d\eta(\theta)\phi(\xi)d\xi,$$

$$(3.4)$$

where $\eta(\theta) = \eta(\theta, 0)$. Thus, $A = A(0)$ and A^* are adjoint operators.

Owning to $\pm i\omega_0^*\tau_s^*$ are eigenvalues both of A and A^*, we can compute the eigenvector of A corresponding to $i\omega_0^*\tau_s^*$ and A^* corresponding to $-i\omega_0^*\tau_s^*$. Assume that the eigenvector of $A(0)$ corresponding to $i\omega_0^*\tau_s^*$ is $q(\theta) = (1, \Delta_1, \Delta_2, \Delta_3)^T e^{i\omega_0^*\tau_s^*\theta}$,

then $Aq(\theta) = i\omega_0^*\tau_s^*q(\theta)$. The definition of $A(0)$ and $\eta(\theta, \mu)$ yields

$$\begin{pmatrix} -3x_{11}^{*2} - 4x_{11}^* & -1 & 0 & 0 \\ \frac{4+K_{12}}{\tau_0} & -\frac{1}{\tau_0} & -\frac{K_{12}e^{-i\omega_0^*\tau_s^*}}{\tau_0} & 0 \\ 0 & 0 & -3x_{12}^{*2} - 4x_{12}^* & -1 \\ -\frac{K_{21}e^{-i\omega_0^*\tau_s^*}}{\tau_0} & 0 & \frac{4+K_{21}}{\tau_0} & -\frac{1}{\tau_0} \end{pmatrix} q(0) = i\omega_0^*q(0).$$

Thus, we can get

$$\Delta_1 = -3x_{11}^{*2} - 4x_{11}^* - i\omega_0^*,$$
$$\Delta_2 = \frac{4 + K_{12} - (1 + i\tau_0\omega_0^*)(-3x_{11}^{*2} - 4x_{11}^* - i\omega_0^*)}{K_{12}e^{-i\tau_s^*\omega_0^*}},$$
$$\Delta_3 = -3x_{12}^{*2} - 4x_{12}^* - i\omega_0^*.$$

Similarly, the eigenvector of A^* corresponding to $-i\omega_0^*\tau_s^*$ is $q^*(s) = D(1, \Delta_1^*, \Delta_2^*, \Delta_3^*)e^{i\omega_0^*\tau_s^*s}$, then we get

$$\Delta_1^* = \frac{-1}{\frac{1}{\tau_0} - i\omega_0^*},$$
$$\Delta_2^* = (i\omega_0^* - \frac{1}{\tau_0})\Delta_3^*,$$
$$\Delta_3^* = \frac{\tau_0(-3x_{11}^{*2} - 4x_{11}^* + i\omega_0^*) + (4 + K_{12})\Delta_1^*}{K_{21}e^{i\omega_0^*\tau_s^*}}.$$

From (3.4), we get

$$\begin{aligned}\langle q^*(s), q(\theta)\rangle &= \overline{D}(1, \overline{\Delta_1^*}, \overline{\Delta_2^*}, \overline{\Delta_3^*})(1, \Delta_1, \Delta_2, \Delta_3)^T \\ &\quad - \int_{-1}^0 \int_{\xi=0}^0 \overline{D}(1, \overline{\Delta_1^*}, \overline{\Delta_2^*}, \overline{\Delta_3^*})e^{-i\omega_0^*\tau_s^*(\xi-\theta)}d\eta(\theta) \\ &\quad \cdot (1, \Delta_1, \Delta_2, \Delta_3)^T e^{+i\omega_0^*\tau_s^*\xi}d\xi \\ &= \overline{D}(1 + \overline{\Delta_1^*}\Delta_1 + \overline{\Delta_2^*}\Delta_2 + \overline{\Delta_3^*}\Delta_3 + \frac{K_{21}\tau_s^*e^{-i\omega_0^*\tau_s^*}}{\tau_0} \\ &\quad \cdot \overline{\Delta_3^*} + \frac{K_{12}\tau_s^*e^{-i\omega_0^*\tau_s^*}}{\tau_0}\overline{\Delta_1^*}\Delta_2).\end{aligned}$$

Thus, we get

$$\begin{aligned}\overline{D} = &(1 + \overline{\Delta_1^*}\Delta_1 + \overline{\Delta_2^*}\Delta_2 + \overline{\Delta_3^*}\Delta_3 + \frac{K_{21}\tau_s^*e^{-i\omega_0^*\tau_s^*}}{\tau_0}\overline{\Delta_3^*} \\ &+ \frac{K_{12}\tau_s^*e^{-i\omega_0^*\tau_s^*}}{\tau_0}\overline{\Delta_1^*}\Delta_2)^{-1}.\end{aligned}$$

Therefore, it is clear that both $\langle q^*(s), q(\theta)\rangle = 1$ and $\langle q^*(s), \overline{q}(\theta)\rangle = 0$ are satisfied. Let u_t be the solution of (3.3) when $\mu = 0$. Define

$$z(t) = \langle q^*, u_t\rangle, \quad W(t, \theta) = u_t(\theta) - 2Re\{z(t)q(\theta)\}. \quad (3.5)$$

On the center manifold C_0, we get

$$W(t, \theta) = W(z(t), \overline{z}(t), \theta),$$

and

$$W(z(t), \overline{z}(t), \theta) = W_{20}(\theta)\frac{z^2}{2} + W_{11}(\theta)z\overline{z} + W_{02}(\theta)\frac{\overline{z}^2}{2} + \dots \ , \quad (3.6)$$

where z and $\overline{z}$ are local coordinates for center manifold C_0 in the direction of q^* and $\overline{q^*}$. Note that W is real if u_t is real. We only consider real solutions. For solution $u_t \in C_0$ of (3.3), due to $\mu = 0$, we have

$$\begin{aligned}\dot{z}(t) &= i\omega_0^*\tau_s^*z + \overline{q^*}(0)F(0, W(z, \overline{z}, 0) + 2Re\{z(t)q(\theta)\}) \\ &= i\omega_0^*\tau_s^*z + \overline{q^*}(0)F_0(z, \overline{z}).\end{aligned}$$

We rewrite this equation as

$$\dot{z}(t) = i\omega_0^*\tau_s^*z + g(z, \overline{z}),$$

where

$$\begin{aligned}g(z, \overline{z}) &= \overline{q^*}(0)F_0(z, \overline{z}) \\ &= g_{20}(\theta)\frac{z^2}{2} + g_{11}(\theta)z\overline{z} + g_{02}(\theta)\frac{\overline{z}^2}{2} + g_{21}(\theta)\frac{z^2\overline{z}}{2} + \dots \ .\end{aligned} \quad (3.7)$$

From (3.5) and (3.6), we have

$$\begin{aligned}u_t &= (u_{1t}(\theta), u_{2t}(\theta), u_{3t}(\theta), u_{4t}(\theta)) \\ &= W(t, \theta) + 2Re\{z(t)q(\theta)\},\end{aligned}$$

where $q(\theta) = (1, \Delta_1, \Delta_2, \Delta_3)^T e^{i\omega_0^*\tau_s^*\theta}$, then

$$\begin{aligned}u_{1t}(0) &= W^{(1)}(t, 0) + z + \overline{z}, \\ u_{2t}(0) &= W^{(2)}(t, 0) + \Delta_1 z + \overline{\Delta_1}\overline{z}, \\ u_{3t}(0) &= W^{(3)}(t, 0) + \Delta_2 z + \overline{\Delta_2}\overline{z}, \\ u_{4t}(0) &= W^{(4)}(t, 0) + \Delta_3 z + \overline{\Delta_3}\overline{z}, \\ u_{1t}(-1) &= W^{(1)}(t, -1) + ze^{-i\omega_0^*\tau_s^*} + \overline{z}e^{i\omega_0^*\tau_s^*}, \\ u_{2t}(-1) &= W^{(2)}(t, -1) + \Delta_1 ze^{-i\omega_0^*\tau_s^*} + \overline{\Delta_1}\overline{z}e^{i\omega_0^*\tau_s^*}, \\ u_{3t}(-1) &= W^{(3)}(t, -1) + \Delta_2 ze^{-i\omega_0^*\tau_s^*} + \overline{\Delta_2}\overline{z}e^{i\omega_0^*\tau_s^*}, \\ u_{4t}(-1) &= W^{(4)}(t, -1) + \Delta_3 ze^{-i\omega_0^*\tau_s^*} + \overline{\Delta_3}\overline{z}e^{i\omega_0^*\tau_s^*}.\end{aligned}$$

Comparing the coefficients with (3.7), we can yield the following important parameters:

$$g_{20} = 2\overline{D}\tau_s^*[-3x_{11}^* - 2 + \overline{\Delta_2^*}\Delta_2^2(-3x_{12}^* - 2)],$$

$g_{11} = 2\overline{D}\tau_s^*[-3x_{11}^* - 2 + \overline{\Delta}_2^* \Delta_2 \overline{\Delta}_2(-3x_{12}^* - 2)],$

$g_{02} = 2\overline{D}\tau_s^*[-3x_{11}^* - 2 + \overline{\Delta}_2^* \overline{\Delta}_2^2(-3x_{12}^* - 2)],$

$g_{21} = 2\overline{D}\tau_s^* \left[(-3x_{11}^* - 2)\left(W_{20}^{(1)}(0) + 2W_{11}^{(1)}(0)\right) - 3 \right]$
$+ 2\overline{D}\,\overline{\Delta}_2^* \tau_s^* \left[(-3x_{12}^* - 2)\left(W_{20}^{(3)}(0)\overline{\Delta}_2 + 2W_{11}^{(3)}(0)\Delta_2\right) - 3\Delta_2^2\overline{\Delta}_2 \right].$

Since g_{21} depends on the coefficient $W_{20}(\theta)$ and $W_{11}(\theta)$, we need to compute them. From (3.3) and (3.5), we can get

$$\dot{W} = \dot{u}_t - \dot{z}q - \dot{\overline{z}}\overline{q}$$
$$= \begin{cases} AW - gq(\theta) - \overline{g}\,\overline{q}(\theta), & \theta \in [-1, 0), \\ AW - gq(0) - \overline{g}\,\overline{q}(0) + F_0, & \theta = 0. \end{cases} \quad (3.8)$$

On the other hand, on the center manifold C_0 near the origin, we can obtain

$$\dot{W} = W_z \dot{z} + W_{\overline{z}} \dot{\overline{z}}$$
$$= [W_{20}(\theta)z + W_{11}(\theta)\overline{z}](iw_0^*\tau_s^* z + g(z, \overline{z})) \quad (3.9)$$
$$+ [W_{11}(\theta)z + W_{02}(\theta)\overline{z}](-iw_0^*\tau_s^*\overline{z} + \overline{g}(z, \overline{z})) + \dots .$$

By comparing the coefficients of $\frac{z^2}{2}$ and $z\overline{z}$, we know that

$$(2iw_0^*\tau_s^* I - A)W_{20}(\theta) = \begin{cases} -g_{20}q(\theta) - \overline{g}_{02}\overline{q}(\theta), & \theta \in [-1, 0), \\ -g_{20}q(0) - \overline{g}_{02}\overline{q}(0) + \frac{\partial^2 F_0}{\partial z^2}, & \theta = 0. \end{cases} \quad (3.10)$$

Similarly,

$$-AW_{11}(\theta) = \begin{cases} -g_{11}q(\theta) - \overline{g}_{11}\overline{q}(\theta), & \theta \in [-1, 0), \\ -g_{11}q(0) - \overline{g}_{11}\overline{q}(0) + \frac{\partial^2 F_0}{\partial z\partial\overline{z}}, & \theta = 0. \end{cases} \quad (3.11)$$

We know that for $\theta \in [-1, 0)$,

$$\dot{W}_{20}(\theta) = 2i\omega_0^*\tau_s^* W_{20}(\theta) + g_{20}q(\theta) + \overline{g}_{02}\overline{q}(\theta).$$

Substituting $q(\theta) = q(0)e^{iw_0^*\tau_s^*\theta}$ into (3.10), then we have

$$W_{20}(\theta) = \frac{ig_{20}}{w_0^*\tau_s^*}q(0)e^{iw_0^*\tau_s^*\theta} + \frac{i\overline{g}_{02}}{3w_0^*\tau_s^*}\overline{q}(0)e^{-iw_0^*\tau_s^*\theta} + E_1 e^{2iw_0^*\tau_s^*\theta}, \quad (3.12)$$

where $E_1 = (E_1^{(1)}, E_1^{(2)}, E_1^{(3)}, E_1^{(4)}) \in R^4$ is a constant vector. Similarly, we obtain

$$W_{11}(\theta) = \frac{-ig_{11}}{w_0^*\tau_s^*}q(0)e^{iw_0^*\tau_s^*\theta} + \frac{i\overline{g}_{11}}{w_0^*\tau_s^*}\overline{q}(0)e^{-iw_0^*\tau_s^*\theta} + E_2, \quad (3.13)$$

where $E_2 = (E_2^{(1)}, E_2^{(2)}, E_2^{(3)}, E_2^{(4)}) \in R^4$ is also a constant vector.

Based on (3.10), (3.11), (3.12) and (3.13), we can obtain

$$E_1 = (2iw_0^*\tau_s^* I - \int_{-1}^0 e^{2iw_0^*\tau_s^*\theta}d\eta(\theta))^{-1}F_{z^2}$$
$$= \begin{pmatrix} E_{11} & E_{12} \\ E_{21} & E_{22} \end{pmatrix}^{-1} F_{z^2}, \quad (3.14)$$

where

$$E_{11} = \begin{pmatrix} 2i\omega_0^*\tau_s^* + 3x_{11}^{*2} + 4x_{11}^* & 1 \\ -\frac{4+K_{12}}{\tau_0} & 2i\omega_0^*\tau_s^* + \frac{1}{\tau_0} \end{pmatrix},$$

$$E_{12} = \begin{pmatrix} 0 & 0 \\ \frac{K_{12}e^{-2i\omega_0^*\tau_s^*}}{\tau_0} & 0 \end{pmatrix}, \quad E_{21} = \begin{pmatrix} 0 & 0 \\ \frac{K_{21}e^{-2i\omega_0^*\tau_s^*}}{\tau_0} & 0 \end{pmatrix},$$

$$E_{22} = \begin{pmatrix} 2i\omega_0^*\tau_s^* + 3x_{12}^{*2} + 4x_{12}^* & 1 \\ -\frac{4+K_{21}}{\tau_0} & 2i\omega_0^*\tau_s^* + \frac{1}{\tau_0} \end{pmatrix},$$

and

$$E_2 = -(\int_{-1}^0 d\eta(\theta))^{-1}F_{z\overline{z}}$$
$$= \begin{pmatrix} 3x_{11}^{*2} + 4x_{11}^* & 1 & 0 & 0 \\ -\frac{4+K_{12}}{\tau_0} & \frac{1}{\tau_0} & \frac{K_{12}}{\tau_0} & 0 \\ 0 & 0 & 3x_{12}^{*2} + 4x_{12}^* & 1 \\ \frac{K_{21}}{\tau_0} & 0 & -\frac{4+K_{21}}{\tau_0} & \frac{1}{\tau_0} \end{pmatrix}^{-1} F_{z\overline{z}}, \quad (3.15)$$

where

$$F_{z^2} = \begin{pmatrix} 2\tau_s^*(-3x_{11}^* - 2) \\ 0 \\ 2\tau_s^*\Delta_2^2(-3x_{12}^* - 2) \\ 0 \end{pmatrix},$$

$$F_{z\overline{z}} = \begin{pmatrix} 2\tau_s^*(-3x_{12}^* - 2) \\ 0 \\ 2\tau_s^*\overline{\Delta}_2\Delta_2(-3x_{12}^* - 2) \\ 0 \end{pmatrix}.$$

Thus, $W_{20}(\theta)$ and $W_{11}(\theta)$ can be determined and g_{20}, g_{11}, g_{02}, g_{21} can be expressed. Hence, we can judge property of Hopf bifurcation by three parameters μ_2, β_2, T_2 and compute the following values:

$$c_1(0) = \frac{i}{2\omega_0^*\tau_s^*}(g_{20}g_{11} - 2|g_{11}|^2 - \frac{|g_{02}|^2}{3}) + \frac{g_{21}}{2},$$

$$\mu_2 = -\frac{Re\{c_1(0)\}}{Re\{\lambda'(\tau_s^*)\}},$$

$$\beta_2 = 2Re\{c_1(0)\},$$

$$T_2 = -\frac{Im\{c_1(0)\} + \mu_2 Im\{\lambda'(\tau_s^*)\}}{w_0^*\tau_s^*}.$$

From the conclusion of Hassard et al. [20], we have the conclusion

Theorem 2 μ_2 determines the direction of the Hopf bifurcation, β_2 determines the stability of the bifurcating periodic solution, and T_2 determines the period of the bifurcating periodic solution. Moreover, if $\mu_2 > 0$ ($\mu_2 < 0$), the Hopf bifurcation is supercritical (subcritical); if $\beta_2 > 0$ ($\beta_2 < 0$), the bifurcating periodic solution is stable (unstable); if $T_2 > 0$ ($T_2 < 0$), the period increases (decreases).

4. Numerical simulations

We use some numerical simulation to illustrate the bifurcation analysis. Firstly, we consider the following Epileptor model:

$$\begin{cases} \frac{dx_{11}}{dt} = -x_{11}^3 - 2x_{11}^2 + 1 - z_1 + I_{11}, \\ \frac{dz_1}{dt} = \frac{1}{2857}[4(x_{11} - x_{01}) - z_1], \end{cases}$$

where x_{01} and I_{11} are regarded as the two parameters. We plot a critical curve with respect to these two parameters in Figure 2, which gives the stable region. Moreover, fixing

$$\tau_0 = 2857, K_{12} = 18, K_{21} = -7, x_{01} = -2.6,$$
$$x_{02} = -1.2, I_{11} = 3.1, I_{12} = 3.1,$$

we consider a coupled Epileptor model with the following form

$$\begin{cases} \frac{dx_{11}}{dt} = -x_{11}^3 - 2x_{11}^2 + 1 - z_1 + 3.1, \\ \frac{dz_1}{dt} = \frac{1}{2857}[4(x_{11} + 2.6) - z_1 - 18(x_{12}(t - \tau_1) - x_{11})], \\ \frac{dx_{12}}{dt} = -x_{12}^3 - 2x_{12}^2 + 1 - z_2 + 3.1, \\ \frac{dz_2}{dt} = \frac{1}{2857}[4(x_{12} + 1.2) - z_2 + 7(x_{11}(t - \tau_2) - x_{12})]. \end{cases}$$
(4.1)

The pathological changing of brain tissues always increase or decrease the time lags of signal transmission bidirectionally at the same time. Therefore, we consider a special scenario $\tau_1 = \tau_2$. We can compute the nontrivial equilibrium point P (0.0114, 4.0997, 0.3640, 3.7870) of model (4.1). In the absence of delay, $\tau_1 = \tau_2 = 0$, the

dynamic behaviors of model (4.1) are described in Figure 3, which indicates that P is locally asymptotically stable. Using Matlab software, we can find the unique positive solution $\omega_0^* = 0.3$ in (2.5). Then, we can obtain $\tau_s^* = 2.6$, $c_1(0) = -3.69 - 1.36i$, $\mu_2 = 8.62$, $\beta_2 = -0.85$, $T_2 = -5.41$. Based on the Theorem 2, model (4.1) undergoes a supercritical Hopf bifurcation at the nontrivial equilibrium point P and the bifurcating periodic solution exists for τ_s slightly larger than τ_s^* and the bifurcated periodic solution is unstable, which can be seen in Figure 4. We also plot Figure 5 to present phase map between x_{11} and its delay x_{11}^d. Moreover, we take τ_0 as the parameter and exhibit a critical curve in the plan $\tau_0 - \tau_s$. From Figure 6, we can see that time delay decreases with the increasing of characteristic time scale τ_0. We also consider other cases such as $\tau_2 = 0.5\tau_1, \tau_2 = 2\tau_1$ and $\tau_2 = 4\tau_1$. The periodic solution still exist which can be seen in Figure 7.

5. Discussions

Our theoretical analysis and numerical simulation both show that the increase of time delay between nodes change the network to SLE state through Hopf bifurcation. The bifurcation value τ_s also relies on characteristic time scale of brain tissue τ_0. The increasing of τ_0 will increase the threshold of bifurcation value τ_s. Time delay between nodes of epileptic network is important for understanding the seizure. The seizure onsets are mainly due to the changes of brain tissues, which alter the topology of epileptic network. Early studies using diffusion tensor imaging (DTI) indicated the decrease in fractional anisotropy (FA) of brain regions of patients with epilepsy, which further changed the time delay of signal transmission between brain regions [21]. Study using fMRI showed global increased time lags through all regions of the brain not involved in seizure onset and propagation [18]. Our study show that the stable network may change to SLE state by introducing time delays between nodes, which indicates that time delay is one of the important reasons for seizure onset. Moreover, our analysis shows that the epileptic network of two coupled nodes goes to the SLE state through Hopf bifurcation.

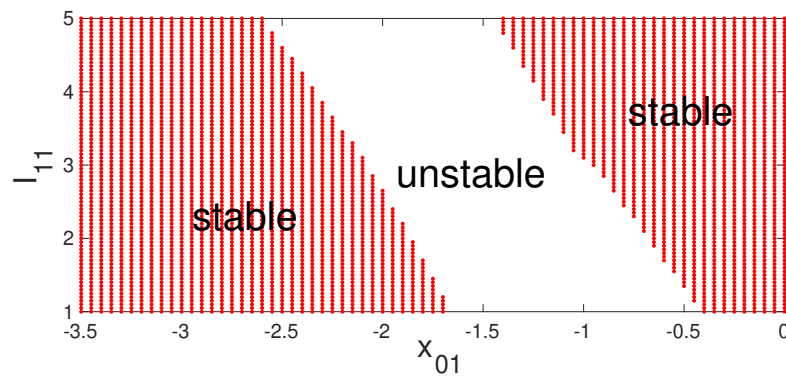Our results support that the brain region with increased

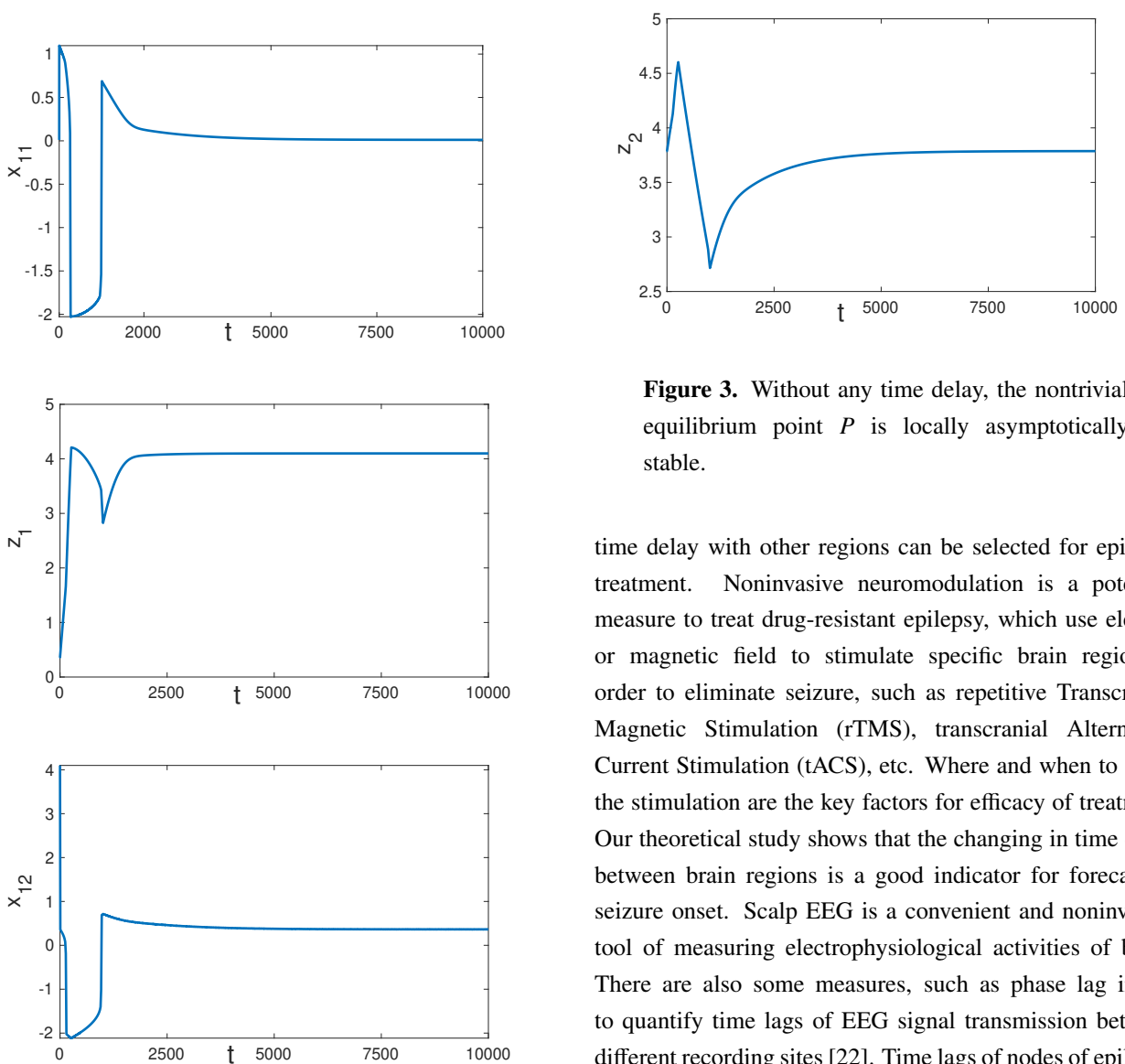**Figure 2.** The stability region in the plane $x_{01} - I_{11}$.

Figure 3. Without any time delay, the nontrivial equilibrium point P is locally asymptotically stable.

time delay with other regions can be selected for epilepsy treatment. Noninvasive neuromodulation is a potential measure to treat drug-resistant epilepsy, which use electric or magnetic field to stimulate specific brain region in order to eliminate seizure, such as repetitive Transcranial Magnetic Stimulation (rTMS), transcranial Alternating Current Stimulation (tACS), etc. Where and when to make the stimulation are the key factors for efficacy of treatment. Our theoretical study shows that the changing in time delay between brain regions is a good indicator for forecasting seizure onset. Scalp EEG is a convenient and noninvasive tool of measuring electrophysiological activities of brain. There are also some measures, such as phase lag index, to quantify time lags of EEG signal transmission between different recording sites [22]. Time lags of nodes of epileptic network can be used to select target for epilepsy treatment.
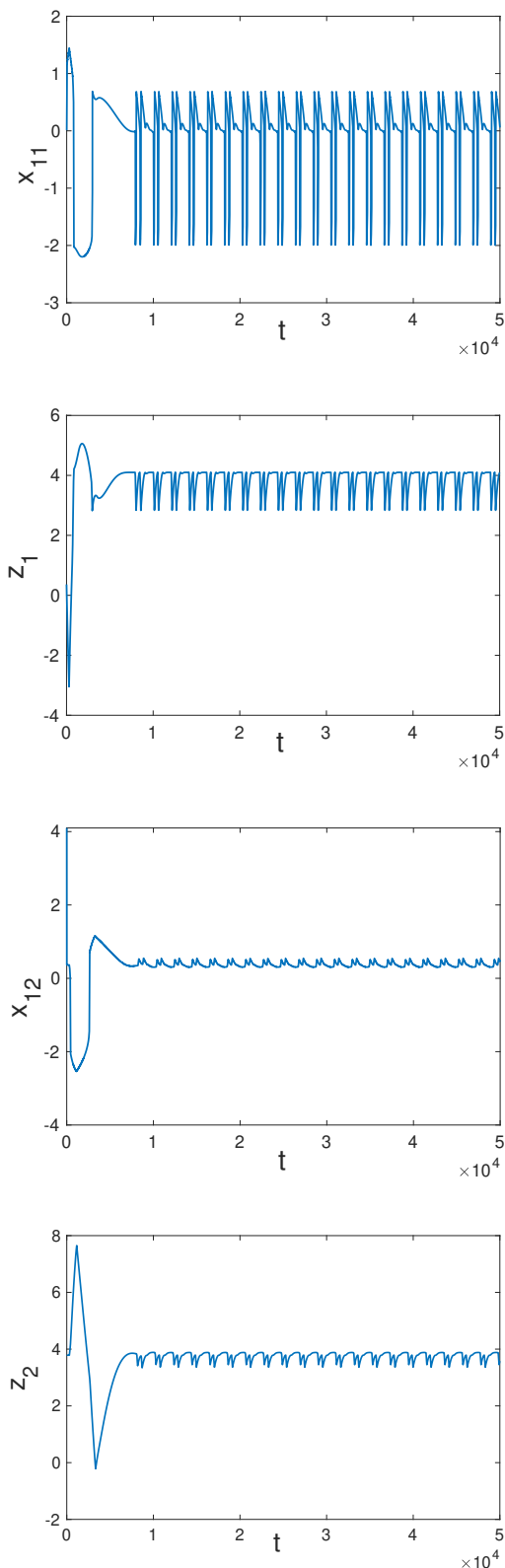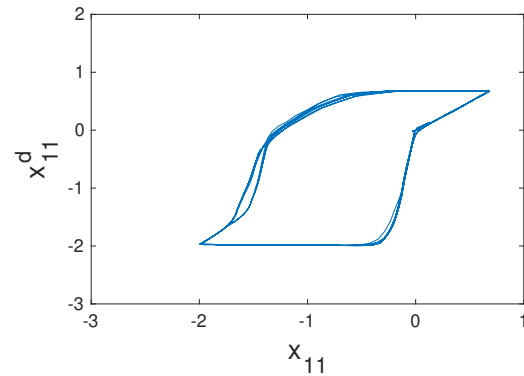
Figure 5. Phase map between x_{11} and its delay x_{11}^d.

Conflict of interest

The authors declared that there is no conflicts of interest in this paper.

References

1. M. Brodie, S. Barry, G. Bamagous, J. D. Norrie, P. Kwan, Patterns of treatment response in newly diagnosed epilepsy, *Neurology,* **78** (2012), 1548–1554. https://doi.org/10.1212/WNL.0b013e3182563b19

2. P. Perucca, F. Dubeau, J. Gotman, Intracranial electroencephalographic seizure-onset patterns: effect of underlying pathology, *Brain,* **137** (2014), 183–196. https://doi.org/10.1093/brain/awt299

3. G. Bettus, E. Guedj, F. Joyeux, S. Confort-Gouny, E. Soulier, V. Laguitton, et al., Decreased basal fMRI functional connectivity in epileptogenic networks and contralateral compensatory mechanisms, *Hum. Brain Mapp.,* **30** (2009), 1580–1591. https://doi.org/10.1002/hbm.20625

4. B. Ridley, C. Rousseau, J. Wirsich, A. Le Troter, E. Soulier, S. Confort-Gouny, et al., Nodal approach reveals differential impact of lateralized focal epilepsies on hub reorganization, *NeuroImage,* **118** (2015), 39–48. https://doi.org/10.1016/j.jprot.2014.11.012

5. J. Premysl, C. Marco, J. John, *Modern concepts of focal epileptic networks,* International Review of Neurobiology, 2014.

Figure 4. A periodic solution of model (4.1) bifurcates from the nontrivial equilibrium point P.
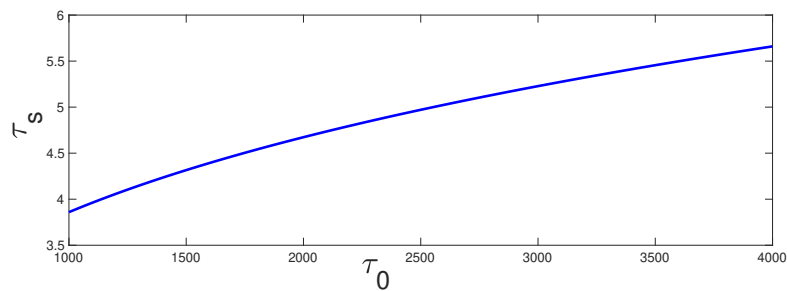
Figure 6. Numerical simulations of the bifurcation value τ_s when varying $\tau_0 \in (1000, 4000)$.

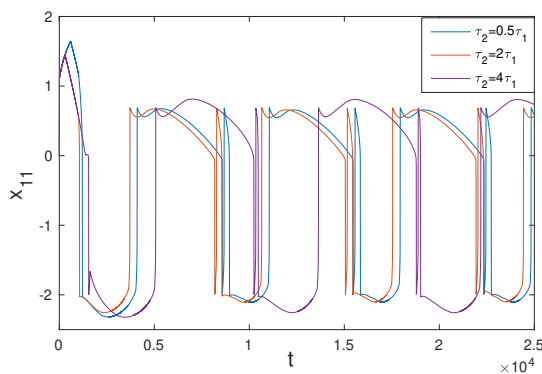**Figure 7.** Solutions of x_{11} when the three differen delays are considered, $(1)\tau_2 = 0.5\tau_1, (2)\tau_2 = 2\tau_1, (3)\tau_2 = 4\tau_1$.

6. D. Cosandier-Rimélé, F. Bartolomei, I. Merlet, P. Chauvel, F. Wendling, Recording of fast activity at the onset of partial seizures: Depth EEG vs. scalp EEG, *NeuroImage,* **59** (2012), 3474–3487. https://doi.org/10.1016/j.neuroimage.2011.11.045

7. M. A. Kramer, W. Truccolo, U. T. Eden, K. Q. Lepage, L. R. Hochberg, E. N. Eskandar, et al., Human seizures self-terminate across spatial scales via a critical transition, *Proceedings of the National Academy of Sciences,* **109** (2012), 21116–21121. https://doi.org/10.1073/pnas.1210047110

8. T. Proix, F. Bartolomei, P. Chauvel, C. Bernard, V. K. Jirsa, Permittivity coupling across brain regions determines seizure recruitment in partial epilepsy, *The Journal of Neuroscience,* **34** (2014), 15009–15021. https://doi.org/10.1523/JNEUROSCI.1570-14.2014

9. M. Ahmadi, D. Hagler, C. McDonald, E. S. Tecoma, V. J. Iragui, A. M. Dale, et al., Side matters: diffusion tensor imaging tractography in left and right temporal lobe epilepsy, *Am. J. Neuroradiol.,* **30** (2009), 1740–1747. https://doi.org/10.3174/ajnr.A1650

10. T. Proix, V. K. Jirsa, F. Bartolomei, M. Guye, W. Truccolo, Predicting the spatiotemporal diversity of seizure propagation and termination in human focal epilepsy, *Nat. Commun.,* **9** (2018), 1–15. https://doi.org/10.1038/s41467-018-02973-y

11. V. Jirsa, K. Jantzen, A. Fuchs, J. S. Kelso, Spatiotemporal forward solution of the EEG and MEG using network modeling, *IEEE T. Med. Imag.,* **21** (2002), 493–504. https://doi.org/10.1109/TMI.2002.1009385

12. F. Wendling, F. Bartolomei, J. Bellanger, P. Chauvel, Epileptic fast activity can be explained by a model of impaired GABAergic dendritic inhibition, *Eur. J. Neurosci.,* **15** (2002), 1499–1508. https://doi.org/10.1046/j.1460-9568.2002.01985.x

13. S. Kalitzin, D. Velis, F. Silva, Stimulation-based anticipation and control of state transitions in the epileptic brain, *Epilepsy Behav.,* **17** (2009), 310–323. https://doi.org/10.3200/DEMO.17.4.310-323

14. P. R. Bauer, R. D. Thijs, R. J. Lamberts, D. N. Velis, G. H. Visser, E. A. Tolner, et al., Dynamics of convulsive seizure termination and postictal generalized EEG suppression, *Brain,* **140** (2017), 655–668.

15. V. K. Jirsa, W. C. Stacey, P. P. Quilichini, A. I. Ivanov, C. Bernard, On the nature of seizure dynamics, *Brain,* **137** (2014), 2210–2230. https://doi.org/10.1093/brain/awu133

16. T. Proix, F. Bartolomei, M. Guye, V. Jirsa, Individual brain structure and modelling predict seizure

propagation, *Revue Neurologique,* **174** (2018), S177. https://doi.org/10.1016/j.neurol.2018.02.047

17. F. Bartolomei, P. Chauvel, F. Wendling, Spatio-temporal dynamics of neuronal networks in partial epilepsy, *Revue neurologique,* **161** (2005), 767–780. https://doi.org/10.1016/S0035-3787(05)85136-7

18. K. Bandt, P. Besson, B. Ridley, F. Pizzo, R. Carron, J. Regis, et al., Connectivity strength, time lag structure and the epilepsy network in resting-state fMRI, *NeuroImage: Clinical,* **24** (2019), 102035. https://doi.org/10.1016/j.nicl.2019.102035

19. H. Zhang, P. Xiao, Seizure Dynamics of Coupled Oscillators with Epileptor Field Model, *Int. J. Bifurcat. Chaos,* **28** (2018), 1850041. https://doi.org/10.1142/S0218127418500414

20. K. Schneider, Theory and Applications of Hopf Bifurcation, Applied Mathematics and Mechanics, *Applied Mathematics and Mechanics,* **62** (1981), 713–714.

21. H. Wang, Y. Huang, D. Coman, R. Munbodh, R. Dhaher, H.P. Zaveri, et al., Network evolution in mesial temporal lobe epilepsy revealed by diffusion tensor imaging, *Epilepsia,* **58** (2017), 824–834. https://doi.org/10.1111/epi.13731

22. L. Peraza, A. Asghar, G. Green, D. M. Halliday, Volume conduction effects in brain network inference from electroencephalographic recordings using phase lag index, *J. Neurosci. Meth.,* **207** (2012), 189–199. https://doi.org/10.1016/j.jneumeth.2012.04.007

AIMS Press